HELICON WAVE PHYSICS IMPACTS ON ELECTRODELESS THRUSTER DESIGN

James Gilland
OAI
22800 Cedar Point Rd.
Brookpark, OH 44142

ABSTRACT

Effective generation of helicon waves for high density plasma sources is determined by the dispersion relation and plasma power balance. Helicon wave plasma sources inherently require an applied magnetic field of .01-0.1 T, an antenna properly designed to couple to the helicon wave in the plasma, and an rf power source in the 10-100's of MHz, depending on propellant choice. For a plasma thruster, particularly one with a high specific impulse (>2000 s), the physics of the discharge would also have to address the use of electron cyclotron resonance (ECR) heating and magnetic expansion. In all cases the system design includes an optimized magnetic field coil, plasma source chamber, and antenna. A preliminary analysis of such a system, calling on experimental data where applicable and calculations where required, has been initiated at Glenn Research Center. Analysis results showing the mass scaling of various components as well as thruster performance projections and their impact on thruster size are discussed.

INTRODUCTION

Electric propulsion thrusters either currently in use (resistojets, arcjets, pulsed plasma thrusters and ion engines) or near realization (MPD thrusters) share a common requirement for electrodes in direct contact with the plasma they generate. The interaction of a hot, high speed fluid with metals both imposes thruster operating lifetime limits and restricts the propellants that might be used. Of course, other propellant properties such as atomic mass and ionization energies, which can determine exhaust velocity and efficiency, also affect propellant choice. The elimination of the electrode-plasma interaction could either increase lifetime with high performance propellants, or allow the use of in-situ propellants such as lunar oxygen. While the use of in-situ molecular propellants may result in lower specific impulse or efficiency, the ability to refuel en route instead of relying on propellants launched from Earth could provide some overall mission benefit.

The electrodeless generation of plasmas implies time-varying fields to remotely induce currents in a gas. Most simply, an inductive coil can be used to generate a plasma. This technique is used in the Radiofrequency Ion Thruster (RIT) thruster concept, but does not eliminate the need for electrostatic grids exposed to the plasma[1]. The inductive method also suffers from its lack of ability to penetrate the plasma beyond the skin depth[2]. By applying a magnetic field to the discharge chamber, a host of plasma waves can be accessed which allow electromagnetic energy to penetrate throughout the plasma and heat it efficiently. One set of plasma waves of interest for electric propulsion is the helicon-electron cyclotron wave. This is the right-hand polarized wave that propagates parallel to a magnetic field at frequencies above the ion cyclotron (ω_{ci}) and below the electron cyclotron (ω_{ce}) frequencies ($\omega_{ci} << \omega << \omega_{ce}$); in an unbounded plasma the wave is called the whistler wave. In bounded magnetized plasmas, the helicon wave is characterized by non-resonant collisional heating of electrons; the cyclotron wave, at $\omega = \omega_{ce}$, resonantly heats electrons in the plane perpendicular to the applied field. This resonant heating introduces the possibility of heating electrons above the Maxwellian temperature of the bulk plasma. This nonthermal energy distribution also has the potential for high I_{sp} operation by expelling these superthermal electrons out of a magnetic nozzle.

Helicon Waves and Sources

Helicon sources have been operated in the laboratory in various gases[3], rf powers ranging from 100 W[4] -10 kWe[5] (Hooper), and magnetic fields from 80 to 2000 G. Typical sources consist of a cylindrical dielectric vacuum chamber located coaxially with applied field coils, and with a copper antenna wrapped around the

outside of the dielectric chamber. Gas is introduced into the chamber and a plasma is created by applying 100-1000 W of rf power to the antenna. These sources have demonstrated the ability to generate high density (n_e ~10^{18}-10^{19} m^{-3}), relatively low temperature (3-5 eV) plasmas. In most of these sources, the aspect ratio (length/diameter) was large, and frequencies were much lower than ω_{ce}[6,7].

At frequencies below one half of ω_{ce}, two possible wave solutions are possible, the helicon/whistler branch and a surface wave branch; at frequencies higher than $\omega_{ce}/2$, a single wave solution, the electron cyclotron wave, exists[8]. The highest densities occur at frequencies well below ω_{ce}, often near the lower hybrid resonance frequency ($\omega_{LH} \approx \sqrt{\omega_{ce}\omega_{ci}}$)[9]. In terrestrial helicon sources, aimed primarily at plasma processing applications, the electron temperatures (T_e) are low, on the order of 3-5 eV[6]. The corresponding ion temperatures are an order of magnitude lower, but might reach 1 eV when operating near the lower hybrid frequency[10]. Conversion of the isotropic electron temperatures to directed axial motion will only produce exhaust velocities on the order of 10 km/s, which is inadequate for most planetary missions[11].

In contrast, ECR heating of plasmas offers the potential for high T_e due to the resonant nature of the wave/particle interaction. ECR waves have often been used to heat plasmas for fusion applications[12] for this reason. The physics of the resonance are well known[13], but the process results in electrons with increased kinetic energy in the plane perpendicular to the applied magnetic field. The deposition of energy into the perpendicular motion of the electrons creates a further benefit for propulsion applications. Conservation of magnetic moment in an adiabatic plasma allows for a plasma with high perpendicular temperature to accelerate in the parallel direction along a diverging magnetic field[13]. The reverse of this behavior is the confinement of plasmas in magnetic mirrors. This conservation allows an ECR thruster to convert temperature to thrust. Previous research has been done in using purely ECR heating for plasma propulsion; however, penetration of ECR frequencies into a plasma proved to be problematic, limited the density in the discharge chamber, and resulted in wall damage from backstreaming ions and electrons[14].

Whistler Dispersion Relation: The dispersion relation gives the dependence of the helicon wave on magnetic field strength and plasma density. The well-known cold plasma dispersion tensor is a first step in defining this dependence. In the Stix notation[15] this tensor is expressed as

$$\begin{bmatrix} S - n_z^2 & -iD & n_z^2 n_\perp^2 \\ iD & S - n^2 & 0 \\ n_z^2 n_\perp^2 & 0 & P - n_\perp^2 \end{bmatrix} \qquad \textit{(1)}$$

Where

$$S = 1 - \frac{\omega_{pe}^2}{\omega^2 - \omega_{ce}^2}, \quad D = -\frac{\omega_{pe}^2 \omega_{ce}}{\omega(\omega^2 - \omega_{ce}^2)}, \quad P = 1 - \frac{\omega_{pe}^2}{\omega^2}$$
$$n_z = \frac{c\,k_z}{\omega}, \quad n_\perp = \frac{c\,k_\perp}{\omega} \qquad \textit{(2)}$$

and $\omega_{pe} = \sqrt{\frac{n_e e^2}{m_e \varepsilon_0}}$ is the electron plasma frequency. The above tensor assumes rectangular coordinates, with the z coordinate defined as the direction parallel to the magnetic field. In the expressions above, ion motion has been neglected, which implies that $\omega >> \omega_{LH} >> \omega_{ci}$, which is reasonable for frequencies of interest in this application. The dispersion relation is found by taking the determinant of the tensor and setting it equal to zero. For a fixed applied wave frequency, the determinant produces a function $D(k_z, k_\perp, n_e, B_0)$ which defines the wave propagation as a function of plasma conditions.

In the thruster application considered here, the magnetic field is formed by a solenoidal coil. The field expands outside of the coil and varies in strength and direction. Similarly, the plasma flowing along the magnetic field lines also expands, resulting in a two-dimensional density field. Low fields in the expansion allow ω to approach ω_{ce}. These conditions differ from most experimental helicon sources, which have radially and axially uniform magnetic fields and axially uniform density distributions, and run at frequencies much lower than ω_{ce}. In these more traditional sources, the dispersion relation is simplified by setting ω/ω_{pe} ~0 and ω/ω_{ce}~0. For an ECR thruster, the ω/ω_{ce} terms must be retained. For an expanding plasma, ω/ω_{pe} also cannot be assumed to be zero. All orders of these two ratios were kept in the dispersion relation derivation.

The dispersion relation was calculated in terms of the variables $\delta = \omega/\omega_{ce}$, k_z, $k_\perp$, and n_e. The full solution to the dispersion relation, solving for k_z or for n_e, for example, results in 2 real roots corresponding to the two branches of the helicon wave. The existence of two solutions is shown in Figure 1, which shows n_e as a function of k_z for fixed $k_\perp$ and different values of δ. Two representative, albeit not ideal, ECR thruster concepts have been considered: a small, narrow source with 2 cm radius, and a larger broad source with radius 10 cm. To calculate the expected density to be achieved in the high field region, the cold plasma dispersion relation was used for wavelengths based on the size of the discharge. In Figure 1, a value of $3.83/a$ was chosen for $k_\perp$, where 3.83 is a zero of the J_0 Bessel equation often seen in calculations of wave radial profiles, and a is the source radius. The existence of two density solutions at low δ and density is more evident in the narrow source example. At fixed density and low δ, two possible k_z options exist. These correspond to the helicon wave in the bulk of the plasma, and an edge localized surface wave[16]. At $\delta \geq 0.5$, only the surface wave can exist, and it is often referred to as the electron cyclotron wave. Propagation in an expanding magnetic field would follow a path in Figure 1 from high density, low δ, low k_z to low density, δ=1, high k_z.

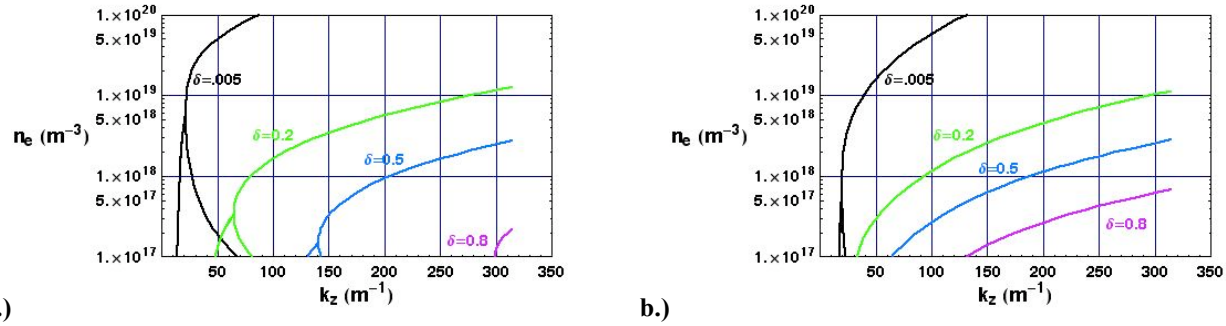

a.) b.)

Figure 1. Solutions to helicon dispersion relation for a range of kz and frequencies. D is ω/ω_{ce}. a.) Narrow (.02 m plasma diameter) source. b.) Broad (0.1 m plasma diameter) source.

Contours of the attainable densities over a range from 10^{17} m^{-3} to 10^{19} m^{-3} are shown in Figure 2 for the two radii considered and for a fixed frequency of 900 MHz. 900 MHz is used because it is the operating frequency of a source soon to be available at NASA Glenn Research Center. In terms of these variables, any variation with respect to frequency is slight. Higher frequencies, however, require higher field strengths (for fixed δ). Figure 2a is the narrow source plot; Figure 2b is the broad source. Density increases upward and to the left; the peak contour is 10^{19} m^{-3}, and the lowest contour is 10^{17} m^{-3}. These plots also give some indication of the requirements for the helicon wave to propagate in a varying magnetic field; as δ increases

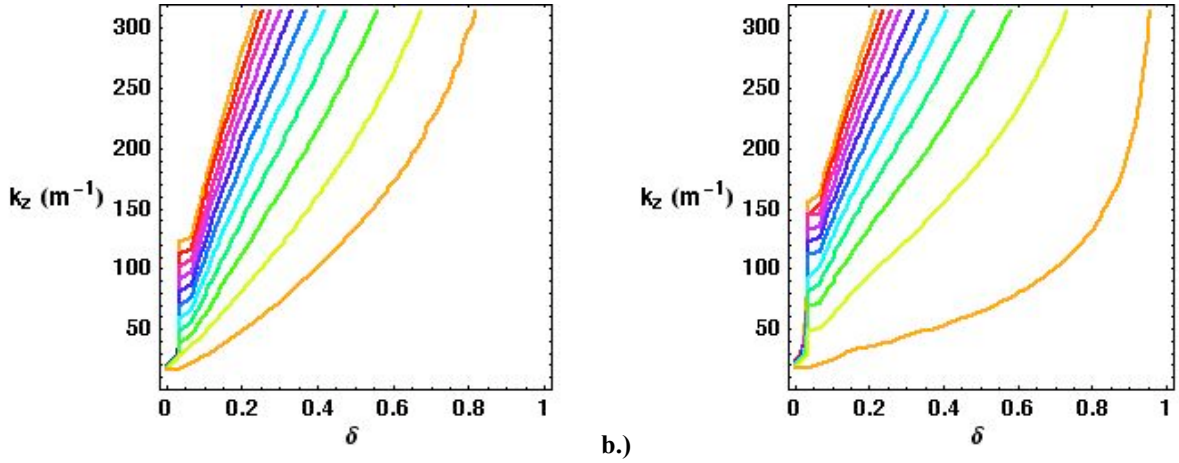

a.) b.)

Figure 2.) Density contours for solution to helicon dispersion relation for two source types. Lowest density contour (10^{17} m^{-3}) is farthest to the right. Highest (10^{19} m^{-3}) is closest to y –axis. a.) Narrow source. b.) Broad source.

(decreasing magnetic field), the density defined by the dispersion relation also decreases. This favors the propagation of the helicon wave to the ECR resonance.

To further assess the potential of helicon to ECR wave propagation, another technique has been used to examine the progress of an initial ray through a varying magnetic and density field. The determinant of the

dispersion relation can be configured to calculate the change of position in physical and **k** space[15]. The relationship gives ray trajectories as coupled differential equations in both physical and k space:

$$\frac{d\vec{\mathbf{r}}}{dt} = -\frac{dD/d\vec{\mathbf{k}}}{dD/d\omega}$$
$$\frac{d\vec{\mathbf{k}}}{dt} = \frac{dD/d\vec{\mathbf{r}}}{dD/d\omega} \qquad (3)$$

In essence, a path is followed through the contour space which matches the physical expansion of field and wave. A full calculation of ray propagation in this manner would include azimuthal modes of the plasma wave; however, by assuming an axisymmetric mode of the wave, the ray paths can be calculated more simply. As the axisymmetric mode is a candidate for this thruster concept, the simplified calculations maintain some relevance to the problem. The integration of these ray tracing equations requires specification of the applied magnetic field and densities. The calculation of these fields will be briefly described in the section below.

Helicon/ECR Thruster

To take advantage of both the high density helicon source and the high temperature/exhaust velocity ECR source requires propagating a helicon wave in a plasma that expands along a diverging magnetic field. The frequency used must be lower than the electron cyclotron resonance frequency in the maximum magnetic field region. The helicon wave is launched by an antenna in the high-field region. The high plasma density, low T_e plasma in this region is created by the non-resonant absorption of the helicon wave. The field strength

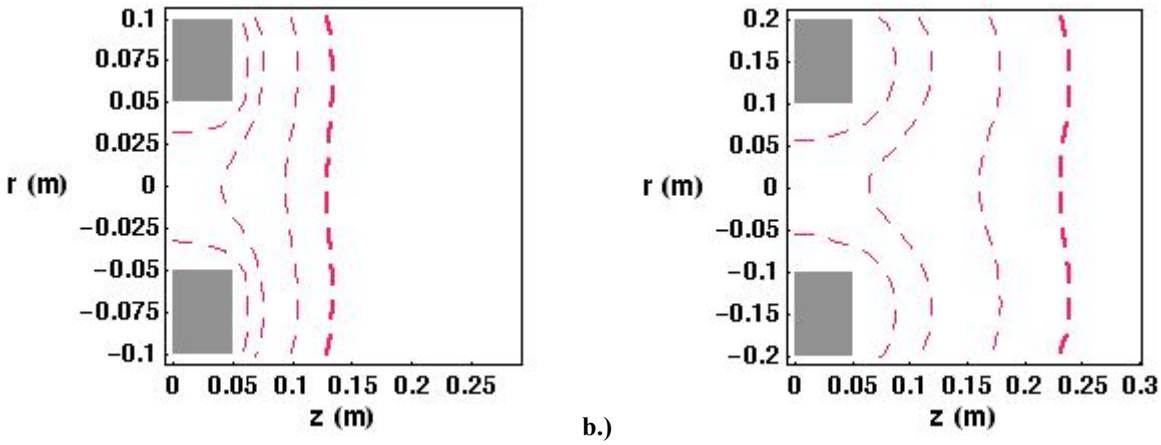

Figure 3. Contours of magnetic field contours normalized by the resonant field for 900 MHz. The bold contour is the resonance location. a.) Narrow (0.02 m diameter) source. b.) Broad (0.1 cm diameter) source.

and density decrease as the field expands, and the helicon wave changes wavelength to continue propagating up to the resonance location, where it is absorbed.

Thruster Applied Magnetic Field: While it is likely that an optimized thruster will require a shaped magnetic field, determining such optimum field shapes will require experimental testing not yet available. For this scaling exercise, a simple solenoidal field was used. For both thruster concepts, a peak field of 0.2 T was selected. For 900 MHz, this allows for a ω_{pe} in the high density region of 0.16, and a resonance field .031 T. An analytical approximation of the solenoidal magnetic field was used to allow for faster calculation. The dimensions of the two coils assumed are given in Table 1. The magnetic field contours for each case are shown in Figure 3, with the cyclotron resonance ($B_{res}=m_e \omega_{rf}/q$) contour in bold.

Thruster Type	Inner Radius a (cm)	Outer radius b (cm)	Length (cm)
Narrow	5	10	10
Broad	10	20	10

Table 1. Chamber/magnet dimensions for the two source geometries considered.

Thruster Density: The density field must also be input to allow an investigation of ray tracing. Expansion of the density in a given magnetic field may be modeled approximately by assuming that mass and magnetic flux are conserved and using a simple energy equation[2]. The model is one dimensional, and

assumes that the plasma flow is purely axial and that density and velocity are constant across the radius of the flow:

$$
\begin{aligned}
& n\,u_z \cdot A = n_0\,u_{z0} \cdot A_0 \\
& B_z \cdot A = B_{z0} \cdot A_0 \\
& n = n_0\, e^{\frac{\Phi q \Phi}{T}} \\
& \frac{M\,u_z^2}{2} + q\Phi = \frac{M\,u_{z0}^2}{2}, \quad u_0 = \sqrt{\frac{qT_e}{M}}
\end{aligned}
\tag{4}
$$

This simple model breaks down where the field, and therefore the plasma, flows radially. The model can be adapted to allow some radial density variation by defining a radial plasma profile at the source, $n_0(r)$. In this paper a Gaussian profile was assumed:

$$
n_0(r,z) = n_0 e^{\frac{\Phi r^2}{w_0^2 \left(\frac{B_z(0,0)}{B_z(z,0)}\right)}} \tag{5}
$$

The profile shape is preserved in the expansion, although the width of the distribution changes with the magnetic field strength. The flow is assumed to be incompressible and the electron temperature (outside of the resonant heating zone) is assumed to be constant. The axial profile of the centerline axial magnetic field strength is shown in Figure 4 for both cases.

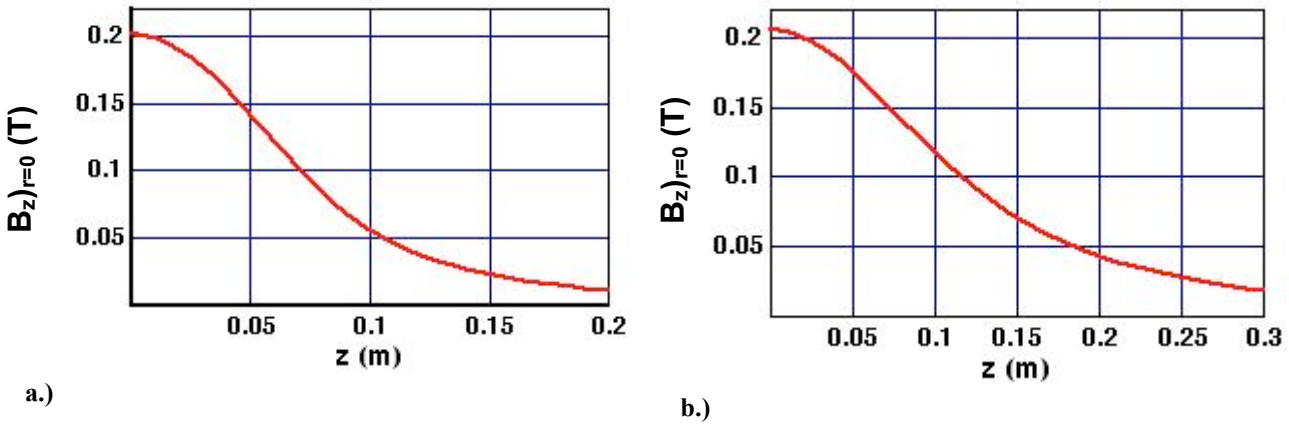

Figure 4. Axial magnetic field profiles used for calculation of expanding plasma density profiles. a.) Narrow source. b.) Broad source.

The calculated density contours for the two cases described are shown in Figure 5. The intersection of finite density contours with the magnet coils is an artifact of not specifying a physical chamber wall due to the simplicity of the current ray tracing code. By choosing initial ray positions near the center of the discharge, the calculated ray paths avoided intersecting the magnetic coils, as will be seen in later calculations.

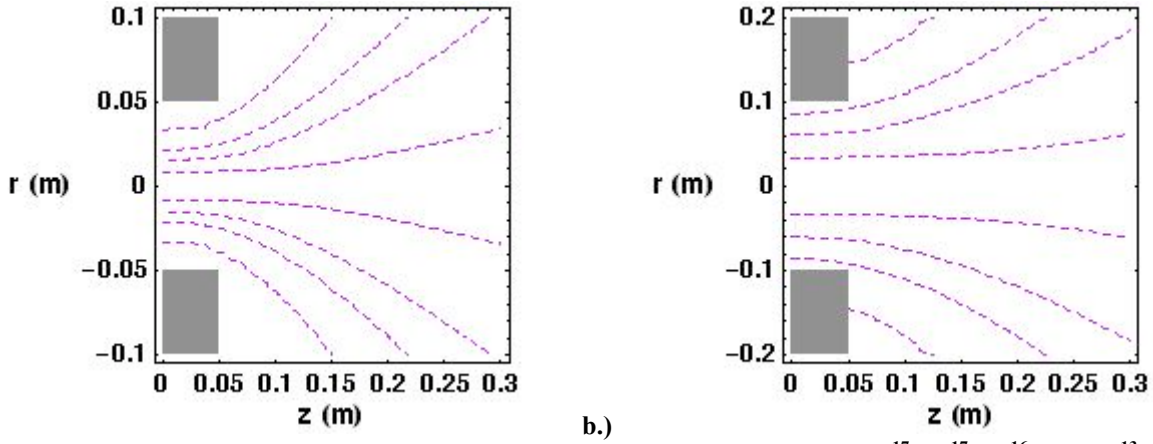

Figure 5 Density contours in expanding magnetic field. Contour values are 5 □ 10^{17}, 10^{17}, 10^{16}, and 10^{13} m^{-3}, with the density decreasing for increasing radius at each fixed position. a.) Narrow source. b.) Broad source.

Helicon wave propagation: With these conditions prescribed, the possibility of helicon wave propagation to an electron cyclotron resonant surface was investigated using ray tracing. Representative initial wave characteristics were chosen based on the basic dispersion relations. Even with the use of the dispersion relation to estimate starting k vectors, a degree of iteration between the dispersion relation (which assumes uniform plasmas) and the plasma density profile was necessary. The profile effects of the radial density distribution meant that the peak density in the Gaussian distribution had to be somewhat higher than the calculation for the uniform density case. For both thruster concepts, the uniform density case required densities on the order of 5 x 10^{17} m^{-3}; the Gaussian distribution required a peak density of 10^{18} m^{-3} to allow the waves to reach the resonance region without diverging into the magnet coil walls.

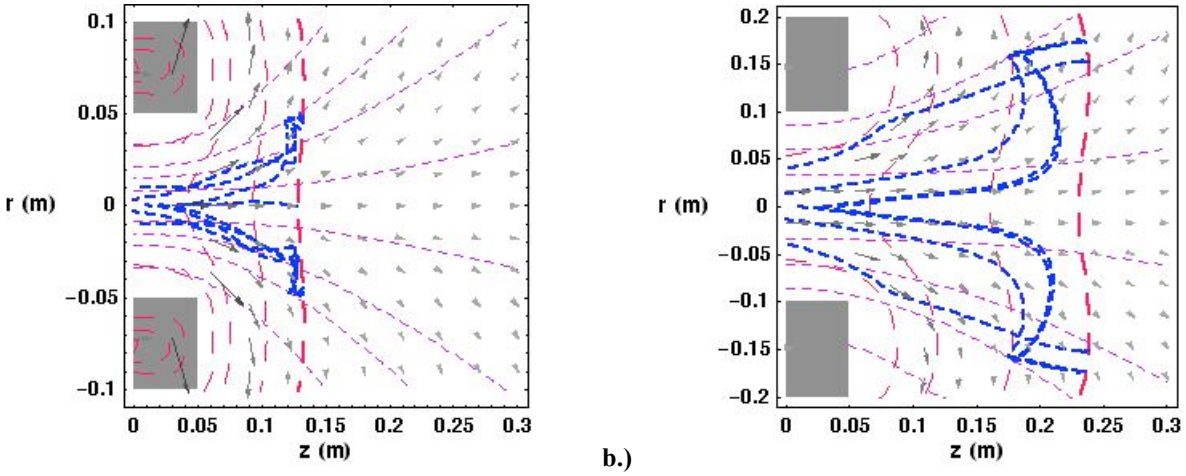

a.) b.)

Figure 6. Ray paths of helicon-ECR waves in helicon source overlayed on magnetic field vectors and contours, and density contours. a.) Narrow source. b.) Broad source.

Ray tracing results for each case are shown in Figure 6, with the rays superimposed over the magnetic field vectors, density and electron cyclotron resonance contours. In both cases, the rays propagate all the way to the resonance region, where they stop, as would be the case for resonant absorption. At resonance, the phase velocity of a wave goes to zero, and the wave is absorbed. At a cutoff, the phase velocity goes to infinity and the wave is reflected. In the narrow source, the rays go almost directly axially until they near the resonance point. In the broader source, the rays turn radially before approaching the resonant location. In fact, some of the rays turn in a radial direction, then flow backwards, moving toward higher magnetic field and lower density regions of the discharge, before reaching a cut off at the low density (10^{16} m^{-3}) edge of the plasma and being reflected toward the resonant surface. In the numerical integration, integration in time past the zero phase velocity resulted in an artificially reflected wave, which is not shown in the ray trajectories of Figure 6.

Ray tracing using a simple cold plasma formulation does not address absorption, either through collisional damping in the case of the helicon, or resonant absorption. A self consistent model of wave propagation and power deposition in a two dimensional magnetic field is beyond the scope of this current report. However, the results indicate the potential for generating a helicon wave that can resonantly heat electrons in a diverging magnetic field. One caveat is that the magnetic field vectors are diverging markedly at the resonance location, particularly in the large area discharge case. This implies that further plasma flow from the resonance location outward would have a significant divergence and suffer a concomitant loss in axial thrust.

Another caveat in considering the ray trajectories superimposed on the input density profile as shown in Figure 6 is that when the heated plasma expands from the resonance zone at higher speeds that the incoming gas, the density will drop proportionately. From the above analysis, where axial magnetic flux $B_z \bullet A_z$ is assumed constant, the flow area of the plasma along the field lines will not change at the resonance location, but the velocity will increase. Mass conservation then requires density to scale inversely with velocity. If the ECR plasma attains the velocities calculated in the simple model used here, the exhaust density will therefore be 0.1 to 0.05 the values calculated for the isotropic plasma expansion. This density drop has not been included in the density contours shown in Figure 6.

Theoretical exhaust velocity: Another aspect of this concept is the acceleration of the plasma to adequate velocities applicable to propulsion. The expansion of an isotropic plasma in an expanding

magnetic field was described previously for plasma flow up to the resonant surface. A similar model for a plasma with high perpendicular energy from resonant heating can also be developed. The energy conservation equation is adapted to account for the perpendicular energy term. The expansion of an anisotropic temperature distribution includes an adiabatic invariant, the magnetic moment[17], $\mu = \frac{qT_\perp}{B}$:

$$
\begin{aligned}
& n\,u_z \cdot A = n_0\,u_{z0} \cdot A_0 \\
& B_z \cdot A = B_{z0} \cdot A_0 \\
& n = n_0\, e^{\frac{\Phi q}{T}} \\
& \frac{M\,u_z^2}{2} + \mu B + q\Phi = \frac{M\,u_{z0}^2}{2} + \mu B_0, \quad u_0 = \sqrt{\frac{qT_e}{M}}
\end{aligned}
\qquad \textit{(6)}
$$

The two regimes of plasma expansion can be combined to examine the possible achievable exhaust velocities. The results of this combined analysis are shown in Figure 7 for both thruster types. Since the heating of the discharge has not yet been analyzed, two perpendicular electron temperatures after resonant absorption ($T_\perp$) were assumed: 50 eV and 100 eV. The potential velocities reached after further expansion along the magnetic field are on the order of 65 and 110 km/s. The terminal velocity in the narrow source is reached by 0.3 m downstream from the center of the magnet coil; the broad source requires 0.5 m to reach its maximum velocity.

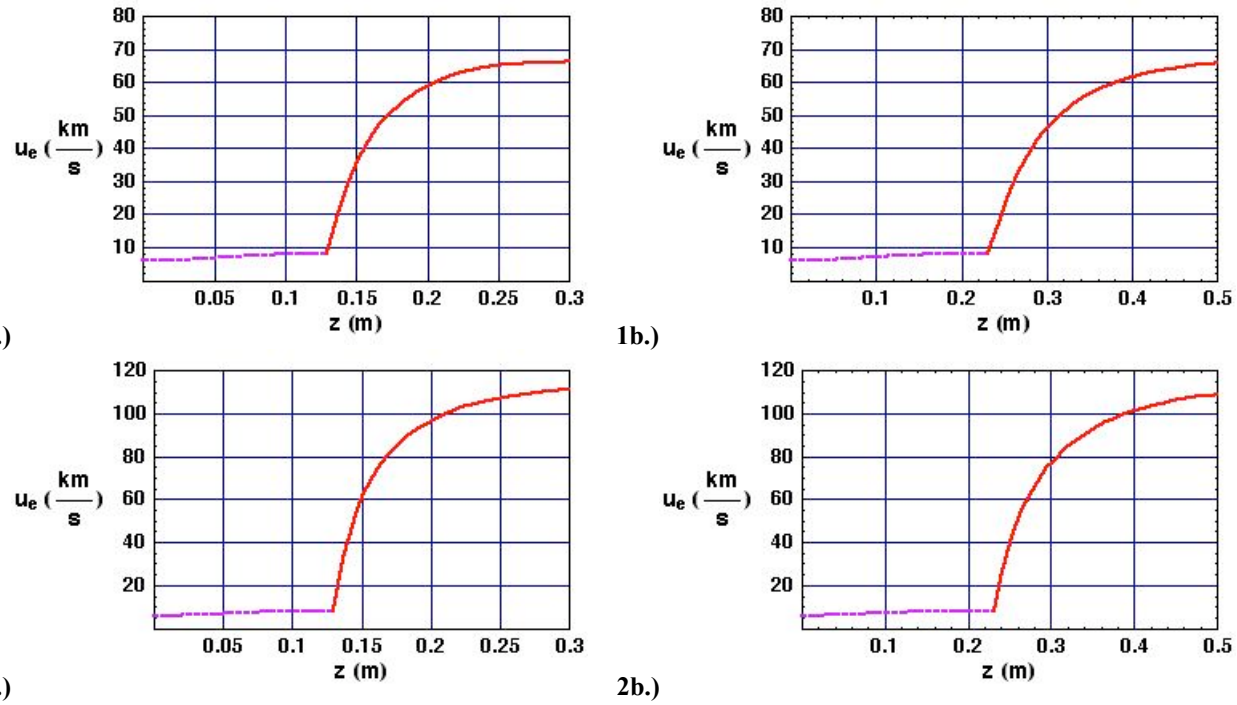

Figure 7. Approximate ideal plasma exhaust velocities for the two source designs and assuming two peak electron temperatures at resonance. 1. $T_\perp$=50 eV a.) narrow source b.) broad source. 2. $T_\perp$=100 eV a.) narrow source b.) broad source.

DISCUSSION OF RESULTS

The possibility of using a helicon-to-ECR wave to produce and heat plasmas for propulsion has been assessed using some fundamental and simplified models of the wave physics. Some basic aspects of this concept appear to be feasible, and show the potential for high u_e operation, in the 50-100 km/s range. These results rely on an initial, simplified (one-dimensional) model of plasma flow combined with a more robust two-dimensional wave propagation analysis. By examining two arbitrary but representative thruster and magnetic field designs, some design issues for an effective ECR thruster have also been revealed.

Wave Propagation

Although helicon/ECR wave propagation appears possible in both the narrow and broad thruster cases, the relative expansion (decrease) of the magnetic field and the plasma density creates differing propagation

paths. The initial conditions of density and **k** vector at the middle of the solenoid, are the same for both cases; however, the broader source has a commensurate wider magnet bore and different field profiles. In the case of the narrow source, waves that start in the small bore magnet propagate primarily axially to the resonant point, resulting in energy deposition in a small, relatively high density region of the discharge. The density at the resonance position is from 1 x 10^{17} to 5 x 10^{17} m^{-3}, and the rays are absorbed in a region whose radial extent is comparable to the magnet bore radius.

The rays in the broader source diverge more strongly in the radial direction, to the point of reflecting backward for a period before resuming propagation in the positive axial direction. Helicon waves are inherently parallel waves and must follow the applied field lines. The broad source suffers from greater radial divergence of the field before the resonant surface, and the ray trajectories indicate this. The rays are not able to turn axially until the density nears its cut off value, changing the nature of the wave and allowing for propagation in the positive z direction. In general, the effects of magnetic field are more pronounced than the density over most of the plasma for two reasons: 1.) the ratio ω/ω_{ce} is greater than ω/ω_{pe}, except at the edge. 2.) ω_{pe} varies as the square root of density, so that the dependence on density is not as strong as the dependence on magnetic field. Straighter field lines up to the resonance or lower densities would be required to have the broad source operate in a manner comparable to the narrow source. One possibility would be to have a second trim coil of larger diameter following the first solenoid, to lessen the radial field components near the center of the plasma. Further design studies will require more robust computational techniques than used in this initial effort.

Thruster Performance

For the assumed heating temperatures at the ECR resonance, using the simplified one dimensional expansion analysis described, both thrusters achieved exhaust velocities of 50-100 km/s for the $T_{e\perp}$ values assumed. However, the one dimensional analysis assumes that the magnetic fields are primarily axial, which is not necessarily true for both source designs. A calculation of the angle of the magnetic field with respect to the axis at the resonance point for each source shows that for the narrow source, the field is at 30-45° to the axis. For the broad source, the angle at resonance is 80°. The divergence efficiency correction for an angle θ is $\eta_d = 1 + \cos(\theta)/2$; the efficiency based on the angle at resonance would be 0.85-0.93 for the narrow source, and 0.59 for the broad source. The effective u_e with these numbers drops to 42-93 km/s for the narrow source, and 29-58 km/s for the broad source. This is still optimistic, because it neglects further divergence along the field beyond the resonance point.

Thruster Mass and Performance Estimates

Thruster Power: Because of the unknowns in calculating heating, plasma confinement, plasma expansion and plasma detachment downstream of the ECR region, thruster efficiency cannot currently be estimated. Previous estimates of power requirements for these devices using hydrogen propellant gave power levels from 1 to 10 kW, with the lower power levels corresponding to the narrow source and the higher levels to the broad source. These estimates were based on the ionization power required to maintain the desired plasma density at the midpoint of the magnet.

Thruster Mass: Conceptually, an ECR thruster would consist of a dielectric tube 0.04 - 0.1 m in diameter, an antenna made of copper wire or strap, and a 0.2 T magnetic field coil. Of these, the dominant mass is the coil. An estimate of the coil mass was made based on applied field coil models developed for applied field MPD thruster conceptual designs[18]. The models assumed hyperconducting aluminum coil operating at liquid hydrogen temperatures and regeneratively cooled by the hydrogen propellant. The maximum allowable current was 2000 A. The coil dimensions correspond to the values given in Table 1. The model yields a mass of 12.9 kg for the narrow source, and 31.9 kg for the broad source. The power levels assumed were commensurate with a 20 kW thruster operating at 50 km/s, and the magnets were sized to allow adequate cooling by the propellant flow rate of approximately 10 mg/s. Thruster specific masses would then be approximately 0.6 kg/kW for the narrow source, and 1.5 kg/kW for the broad source.

FURTHER WORK

Full analysis of a helicon-ECR thruster must take into account multiple, interrelated facets:

1. Wave dispersion in spatially varying magnetic and density fields
2. Self consistent wave absorption/plasma heating
3. Plasma expansion

4. ECR heating including collisional dissipation
5. Plasma detachment from expanding magnetic field lines

The models presented herein only take into account the first facet, and partially the third. It is important to remember that the existence of a helicon-wave-generated plasma is assumed in order to provide the conditions for the ray tracing calculations. Coupling between the antenna and plasma, while implied by the initial dispersion relation calculations, has not been demonstrated to generate the plasma densities assumed. This involves more detailed antenna design as well as experimental verification. Some analysis of the effects of collisions on the resonantly heated electrons should be possible, and has often been done in regard to fusion applications. However, the self consistent heating and propagation phenomena will probably be best approached via experiment. Similarly, the detachment of the plasma from the magnetic field will require experiments to fully demonstrate its feasibility.

With these caveats in mind, preliminary analyses show that a helicon-ECR thruster offers the possibility of electrodeless, high exhaust velocity electric propulsion. These analyses also indicate some initial design guidelines for effective magnetic field shaping to match the thruster conditions to the desired wave propagation and absorption. Narrow helicon sources appear to provide more effective plasma utilization and better expansion properties for propulsion; a broader source requires magnetic field shaping, possibly through the use of a second trim coil, to produce high temperature plasmas in a magnetic field region suitable for expansion to high exhaust velocity. Conceptual hydrogen thruster designs with regeneratively cooled hyperconducting magnets show specific mass values of 0.6-1.5 kg/kW at the 20 kW level.

REFERENCES

[1]K. H. Groh and H. W. Loeb, "State of the art radio-frequency ion sources for space propulsion," Rev. Sci. Instrum. **65** (5), 1994.

[2]M. A. Lieberman and A. J. Lichtenberg, Principles of Plasma Discharges and Materials Processing, Wiley and Sons, NY 1994. p. 429.

[3]A. J. Perry, D. Vender, and R. W. Boswell, "The application of the helicon source to plasma processing," J. Vac Sci. Technol. B **9** (2), 1991.

[4] F. F. Chen, "Experiments on helicon plasma sources," Phys. Plasmas **6** (3), 1999.

[5]B. W. Stallard, E. B. Hooper, and J. L. Power, "Plasma confinement in the whistler wave plasma thruster," J. Prop. And Power **17** (2): 433-440 MAR-APR 2001.

[6] J. Gilland, R. Breun, and N. Hershkowitz, "Neutral pumping in a helicon discharge," Plasma Sources Sci. Technol. **7** (3) 1998.

[7] P. Zhu, and R. W. Boswell, "ArII Laser Generated by Landau Damping of Whistler Waves at the Lower Hybrid Frequency," Phys. Rev. Lett. **63** (26) 1989.

[8] Chen, F. F. "Physics of Helicon Discharges," Phys. Plasmas **3** (5) May 1996.

[9] Boswell, R. W. "Very efficient plasma generation by whistler waves near the lower hybrid frequency," Plasma Phys. Controlled Fusion, **26** (10), 1984.

[10] J. F. Kline, et al., "Slow wave ion heating in the HELIX helicon source," Plasma Sources Sci. Technol. **11** (2002) pp. 413-425.

[11] J. H. Gilland, "Mission and System Optimization of NEP Vehicles for Lunar and Mars Missions," IEPC Paper No. 91-038, 1991.

[12] Y. Tatematsu et al., "Electron cyclotron resonance heating near the turning point in inhomogeneous magnetic field," Phys. Plasmas **3** (9), 1996.

[13] F. Chen, Introduction to Plasma Physics, Plenum Press, New York, 1984.

[14] J. Sercel, "ECR Thruster Research – Preliminary Theory and Experiments," AIAA Paper No. 89-2379, July, 1989.

[15] T. H. Stix, Waves in Plasmas, AIP, NY, NY 1992. pp 7-37.

[16]G. G. Borg and R. W. Boswell, "Power coupling to helicon and Trivelpiece-Gould modes in helicon sources," Phys. Plasmas. **5** (3) 1998.

[17] Plasma-flow resulting from electron-cyclotron-resonance heating on a magnetic hill," Hooper EB Phys. Plasmas **2** (12): 4563-4569 Dec. 1995.

[18] J. H. Gilland, R. M. Myers, and M. J. Patterson, "Multimegawatt Electric Propulsion System Design Considerations," AIAA Paper No. 90-2552, 1990.